Rooting Meta-ecosystems with Reciprocal Lateral Carbon and Nitrogen Flows in a Yangtze Coastal Marsh

Yu Gao , Bin Zhao * , Neil Saintilan , Wanben Wu , Maina Mbui , Li Wen , Feng Zhao , Tao Zhang , Zhi Geng , Gang Yang , Chao Song , Ping Zhuang *

Posted Date: 1 October 2023

doi: 10.20944/preprints202310.0015.v1

Keywords: coastal wetland; carbon; nitrogen; coupling; stoichiometry; meta-ecosystem

Article

Rooting Meta-Ecosystems with Reciprocal Lateral Carbon and Nitrogen Flows in a Yangtze Coastal Marsh

Yu Gao [1,2,3,4], Bin Zhao [2,*], Neil Saintilan [3], Wanben Wu [2,5], Maina Mbui [3], Li Wen [6], Feng Zhao [1], Tao Zhang [1], Zhi Geng [1], Gang Yang [1], Chao Song [1] and Ping Zhuang [1,*]

1 East China Sea Fisheries Research Institute, Chinese Academy of Fishery Sciences; Key Laboratory of Fisheries Remote Sensing, Ministry of Agriculture and Rural Affairs; Scientific Observing and Experimental Station of Fisheries Resources and Environment of East China Sea and Yangtze Estuary, Shanghai 200090, China
2 Ministry of Education Key Laboratory for Biodiversity Science and Ecological Engineering, Coastal Ecosystems Research Station of the Yangtze River Estuary, and Institute of Eco-Chongming (IEC), Fudan University, Shanghai 200438, China
3 School of Natural Sciences, Macquarie University, Sydney, NSW 2109, Australia
4 Key Laboratory of Yangtze River Water Environment, Ministry of Education, Tongji University 200092 Shanghai, China
5 Center for Ecological Dynamics in a Novel Biosphere (ECONOVO), Department of Biology, Aarhus University, Aarhus 8000, Denmark
6 Department of Planning, Industry and Environment, Parramatta, NSW 2150, Australia
* Correspondence: zhaobin@fudan.edu.cn (B.Z.); pzhuang@ecsf.ac.cn (P.Z.)

Abstract: The dynamics of hydrological lateral nutrient fluxes contribute to our understanding of ecological functions related to energy, materials, and organism flows across various spatiotemporal scales. To explore the connectivity between multiple spatial flow processes, we conducted a one-year field measurement to assess lateral hydrologic carbon (C) and nitrogen (N) fluxes over the continental shelf in the Yangtze estuary. We observed a significant correlation between the differences in remote sensing-based estimates of gross primary production (GPP) (ΔGPP_{MODIS}) and the differences in eddy covariance (EC) tower-based GPP (ΔGPP_{EC}) at both high-elevation and low-elevation sites. Over the course of a year, our predicted daily maximum tidal elevation (TE) closely matched the observed values in the creek, which facilitated the development of theoretical models to simulate biogeochemical cycling processes and aquatic ecosystem functions. Our findings indicate that the studied saltmarsh acts as a net exporter of dissolved total C (DTC) while serving as a net sink for dissolved total N (DTN). Furthermore, there is a significant correlation in the total dissolved stoichiometry of the C/N ratio between imports and exports. These findings highlight the importance of integrating ecological stoichiometric principles to gain a deeper understanding of the complex relationships between physical, chemical, and biological processes, particularly within the context of the meta-ecosystem framework. Additionally, when considering reciprocal hydrological lateral C and N flows, single ecosystem can function both as sources and sinks within the meta-ecosystem framework.

Keywords: coastal wetland; carbon; nitrogen; coupling; stoichiometry; meta-ecosystem

1. Introduction

The terrestrial-aquatic continuum is tightly interconnected through energy, material, and organism flows across various spatiotemporal scales (Casas-Ruiz et al., 2023). The hydrological processes profoundly influence carbon (C) cycling as well as nitrogen (N) exchange (Gao et al., 2020). At the landscape scale, these varied flows can be regulated by lateral hydrological fluxes, which in

turn modify the underlying biogeochemical landscape (Wang et al., 2023). Recent studies have demonstrated the growing recognition of the hydrological C and N fluxes importance for regional nutrient budgets, as highlighted in nutrient cycling (Leroux et al., 2017). Importantly, although continental margins comprise less than one-fifth of the world ocean's surface area, their contribution to C and N biogeochemical cycles is equally critical as that of the deep sea (Sandoval-Gil et al., 2019). Thus, the terrestrial-aquatic continuum concept reveals the importance of hydrologic processes in transporting nutrients between ecosystems (Hillman et al., 2018). The movement of matters from one ecosystem to another underscores the importance of connectivity in sustaining and regulating the energy balance and material cycling processes in transition zones (Regnier et al., 2022). For example, the lateral C/N flows provide nutritional value to various aquatic consumers, including fish, and are critical in transferring nutrients between different ecosystems within the terrestrial-aquatic continuum (Taillardat et al., 2019). Understanding the composition and transport of C and N in tidal flows is crucial, not only for practical purposes such as quantifying tidal import/export fluxes but also for advancing theoretical models that simulate biogeochemical cycling processes and aquatic ecosystem functions in a more nuanced manner (Gao et al., 2014). Thus, a comprehensive understanding of lateral mass exchange processes can enhance our knowledge of the ecological importance of coastal ecosystems across various temporal and spatial scales (Clark et al., 2020).

The evidence supporting the use of stoichiometric ratios (e.g., C/N ratio) in modeling basic biogeochemical patterns has been growing and includes examples from the terrestrial-aquatic continuum (Marleau et al., 2015). The analysis of stoichiometric ratios can serve as a valuable indicator of the relocation and redistribution of nutrients between adjacent ecosystems in the landscape (Harvey et al., 2023). It can also help elucidate the driving behind spatial variations in fundamental nutrient transport (Gülzow et al., 2018). For example, there is growing evidence indicating that the interaction between terrestrial and aquatic systems supplies energy (C) and nutrients (e.g., N) to heterotrophic bacteria and certain algae, which may potentially contribute to coastal hypoxia (Das et al., 2011) and eutrophication (Makings et al., 2014). Additionally, increasing modeling assessments and field investigations have provided evidence for coastal wetland management and regional C/N ratio estimation in the context of uncertainties related to human activities and climate change (McGroddy et al., 2008). Nevertheless, it remains uncertain how lateral mass exchange facilitates the transport of nutrients with varying C/N ratios from terrestrial to marine systems, particularly during spring tides and heavy rainfall events (Jeong et al., 2023). Environmental scientists have explored these effects while incorporating remote sensing observations and field measurements to assess and validate regional nutrient budgets, albeit in a somewhat fragmented manner (Regier et al., 2021). For example, in our previous study, we calculated the annual C budget of a coastal wetland using tower-based measurements and time-series data from the Moderate Resolution Imaging Spectroradiometer (MODIS) (Yan et al., 2008). We also carried out continuous field observations of the lateral detritus flux in the coastal wetland to identify and measure the most critical component of the hydrologic nutrient budget (Gao et al., 2018). However, it appears that only a limited amount of quantitative data has been published regarding bidirectional hydrologic nutrient transport, even though the absence of such data have been acknowledged in previous years (Covino 2017). We still lack a comprehensive understanding of how spatial patterns in hydrological stoichiometry influence biogeochemical processes and the tools needed to predict the effects of global changes on these processes (Li et al., 2022).

Fortunately, the development of a meta-ecosystem framework provides a powerful theoretical tool to understand spatial flows of energy, materials and organisms across ecosystem boundaries (Gravel et al., 2010). It presents a new perspective for thoroughly exploring the mechanisms that connect nutrient flows at all levels across various spatial scales, thereby upgrading and unifying it into a spatial ecology framework (Marleau et al., 2020). In our previous, we also found that the relatively large amount of suspended silt and sedimentation largely offset the C export by the macrodetritus and led to a near neutral source of lateral flux C budget (Gao et al., 2023). However, the previous study lacked specific information about lateral hydrologic nutrient (i.e., N) flows. To explore the possibility of connecting multiple spatial flow processes, we conducted a one-year

Preprints (www.preprints.org) | NOT PEER-REVIEWED | Posted: 1 October 2023 doi:10.20944/preprints202310.0015.v1

intensive and comprehensive field measurement campaign to assess the lateral hydrologic C and N fluxes over the continental shelf in the Yangtze estuary. We aimed to address the following questions: 1. What are the relative contributions of the lateral hydrologic C and N fluxes in the marsh C and N budgets? 2. What is the seasonal variability of the hydrologic C and N fluxes? 3. To what extent do these C and N fluxes and their budgets respond to spatial variability, with emphasis on dissolved total carbon (DTC) and cross-shelf export of dissolved total nitrogen (DTN)? While detritus transport and sedimentation have been thoroughly examined in our earlier study (Gao et al., 2020), the focus here was on the dynamics of hydrologic C and N fluxes. The discussion of hydrologic C and N fluxes in the study centered around the seasonal variability and their relationships with the difference between GPP measured by the EC technique (GPP_{EC}) and that measured by remote sensing (GPP_{MODIS}).

2. Materials and methods

2.1. Study area

Our studied wetland is in the Yangtze River estuary (31°25' ~ 31°38'N, 121°50' ~ 122°05'E) and covers an area of 230 km^2 (Figure 1) (Guo et al., 2009). The major vegetation types include native *Scirpus mariqueter* and *Phragmites australis*, as well as the invasive *Spartina alterniflora*. The soil is classified as hydric, with C storage (± SD) in the top 0-20 cm sediment at approximately 3.14 ± 0.05 kg C m^{-2} (Gao et al., 2021). The hydrology of the marsh features a well-developed creek system and receives tidal water from the adjacent coast (Wu et al., 2022). The tides are typically semidiurnal, with the maximum tidal height ranging from 4.6 m to 6.0 m above sea level. During the period of spring tides, most of the wetlands are inundated by seawater (Ouyang et al., 2013). The flow speeds of tides are typically less than 1.0 m/s, but they may reach 2.0 m/s in the main channels, with a maximum recorded speed of 2.45 m/s (Zhao et al., 2008). The climate of the area is characterized by strong seasonal variations, abundant precipitation (606.1~1480.5 mm), and mean monthly temperatures ranging from 2.8~27.5 °C (Huang et al., 2020). The wind direction is typically SSE–SE in the summer, generating a northward longshore current, and NW–NE in the winter, producing a southward longshore current (Gao et al., 2023).

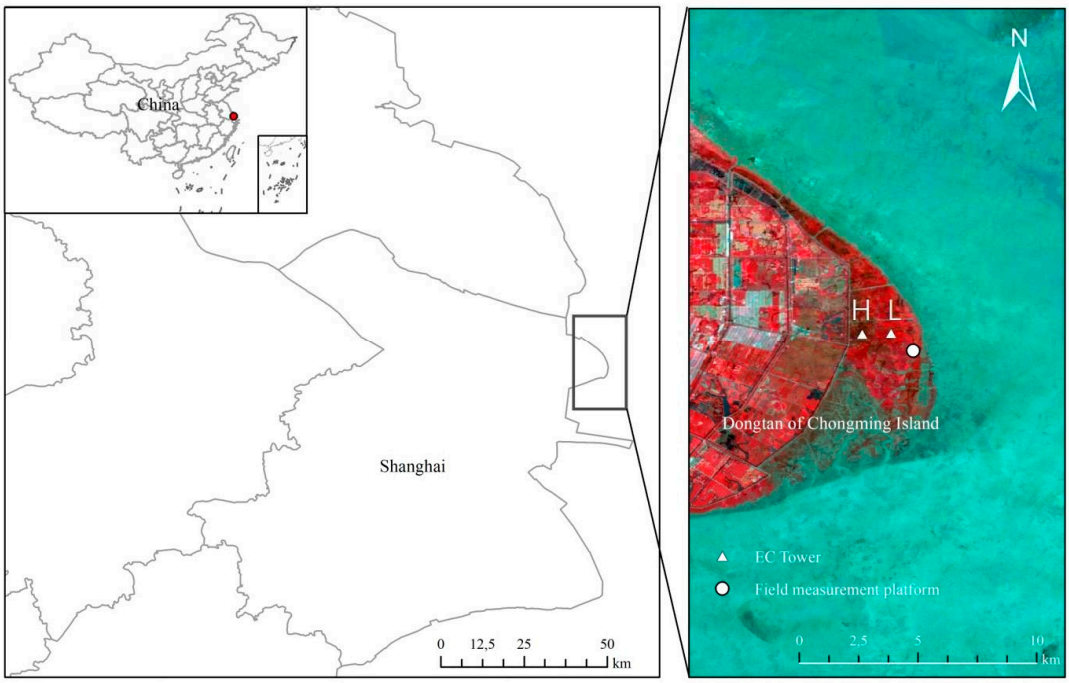

Figure 1. Locations of the field measurement platform (31°30.600'N, 121°58.800'E) and two stations of EC towers (H: high-elevation site, 31°31.000'N, 121°58.300'E; L: low-elevation site, 31°31.014'N, 121°58.300'E) (the background is the synthetic Landsat TM image in 2010).

 doi:10.20944/preprints202310.0015.v1

2.2. Environmental data preparation

2.2.1. Eddy covariance (EC) data

The EC observation system was applied to quantify half-hourly EC flux tower data, including air humidity, air pressure, wind speed, wind direction, PAR, NEE, and GPP (Figure 1). The processing of C flux and auxiliary micrometeorological variables involved several standard quality checks and correction steps (Guo et al., 2009). These eddy covariance data were processed using EddyPro software (v. 7.0.4) (LI-COR Inc., Lincoln, NE, USA), following the workflow outlined in Reichstein et al. (2005) and Chu et al. (2014). For detailed information about the observation instruments and data processing, please refer to Li et al., (2018). The diagnostic signals from a sonic anemometer (CSAT3, CSI), an open-circuit CO_2/H_2O infrared gas analyzer (LI7500A, LI-COR Inc., Lincoln, NE, USA), and an open-circuit CH_4 gas analyzer (LI7700, LI-COR) were used to detect and filter out any periods of instrument malfunction using a dynamic parameter model (Moffat et al., 2007). Environmental condition monitoring was integrated into the EC systems. To ensure data quality, the raw data processing steps were adopted to identify invalid data for quality control (Yang et al., 2023). The daily GPP_{EC} data were then aggregated into 8-day values by fitting the Michaelis–Menten model for subsequent analysis (Gao et al., 2021). These data were obtained starting from January 1, 2005. To align with the measurements of hydrological lateral mass flux, the data from 2010 were utilized in this study.

2.2.2. MODIS products

We downloaded the MODIS tile h28v05 from the website (http://remotesensing.unh.edu/) for the study period in 2010 (Yan et al., 2010). To estimate GPP, we obtained the 8-day MODIS reflectance product (MOD09A1, 500 m) for surface reflectance at a spatial resolution of 500 m to match the footprint of our two EC towers (Figure 1) (Zhao et al., 2009). To fill the missing data, we used the MODIS remote sensing data for landscape-level GPP (GPP_{MODIS}) based on the gap-filled product MOD17A2HGF version 6.1 from the Land Processes Distributed Active Archive Center (LP DAAC) (https://lpdaac.usgs.gov/data_access) (Yang et al., 2023). Due to rapid vegetation succession, sedimentation, and the expansion of *Spartina*, six years after the installation of the two EC towers, the vegetation characteristics in the two sites gradually became more similar (Liu et al., 2020b). For this reason, we conducted a topographical survey to measure elevation variations near the towers. Based on this survey, Dongtan was selected as the model ecosystem in this paper for the study of lateral C and N flows (Gao et al., 2023). Therefore, high-temporal-resolution MODIS datasets and field surveys were combined to analyze this rapid lateral exchange process(Wu et al., 2015). We calculated both the differences in MODIS-based GPP (ΔGPP_{MODIS}) for the two cells covering the footprints of the two flux towers and the differences in GPP from the eddy covariance towers (ΔGPP_{EC}) at the two sites (Gao et al., 2021). This enabled us to study the lateral C flux resulting from tidal activities (Yan et al., 2008).

2.3. Lateral Hydrologic C and N Fluxes

The sampling campaign was designed to select a typical tidal creek that extends from west to east (Figure 1). Lateral hydrologic C and N fluxes were computed based on tidal waves (floods and ebbs) and water C and N concentrations during the ice-free periods of 2010 (Lin et al., 2023). The tidal elevation (TE) was standardized with reference to sea level (Wusong datum) prior to sampling the lateral hydrological C and N fluxes. We calculated surface water discharges by solving the marsh water budget on a tidal scale (Lu et al., 2023b). To collect samples during the complete tidal cycle, the concentrations of C and N in tidal water were manually sampled every hour during tidal periods throughout the year 2010, spanning from January to December (Table 1). Monthly tidal wave sampling was conducted at the sampling platform 2~6 times during the spring tides of each month in 2010 (Figure 1). During the diurnal tide cycle, two 500 ml water samples were simultaneously collected every hour as duplicate samples for the analysis of physical and chemical parameters. In

 doi:10.20944/preprints202310.0015.v1

total, there were 44 sampling trips during the study period. Following collection, the water samples were placed in refrigerators at 4 °C in the field and transported to the lab at Fudan University every two days for subsequent analysis (Lu et al., 2023c).

Table 1. The daily maximal tidal elevation TE (m) for each sampling day in 2010. DOY refers to the day of the year.

DOY	TE (m)	DOY	TE(m)	DOY	TE(m)	DOY	TE(m)
1	0.97	120	1.07	194	1.33	254	1.39
2	1.38	134	1.12	220	1.15	280	1.21
3	1.38	135	1.16	221	1.57	281	1.60
4	1.41	136	1.14	222	1.76	282	1.31
31	1.38	163	1.33	223	1.63	283	1.29
32	1.38	164	1.38	224	1.48	310	1.29
33	1.09	165	1.33	225	1.36	311	1.25
60	1.39	166	1.19	250	1.60	312	1.25
61	1.21	167	1.06	251	1.58	313	1.12
62	1.24	192	1.35	252	1.60	340	0.99
119	0.97	193	1.40	253	1.48	341	0.80

Water samples were transported to the laboratory, where they were filtered under a vacuum through precombusted (6 hours at 450 °C) and preweighed Whatman GF/F filters (0.7 μm). DTC and DTN were determined using an elemental analyzer (Multi N/C 3100 with solid module HT1300, Analytik Jena AG, Germany). During the determination process, each sample was injected in parallel 3~5 times, with a relative standard deviation of less than 2%. Blank controls were implemented by processing distilled water samples using identical procedures. If the concentration fell within the reference range, the subsequent sample analysis and determination could proceed. The precision of the analysis, determined by repeatedly sampling 10% of the samples, yielded a relative error of less than 5%. For a more comprehensive description of the procedures employed, please refer to Gao et al., (2023). The concentration of C and N in each water sample was utilized to calculate C/N ratios, expressed as molar ratios.

2.4. Statistical Analysis

All data were subjected to testing for both homogeneities of variance and normality of distribution using Levene's test and the Kolmogorov–Smirnov test, respectively. No data transformation was necessary to achieve normal distribution or homogeneity. Statistical tests and model fittings were conducted using the R programming language (R Development Core Team, 2017, version 3.4.3). Unless stated otherwise, the significance level was set at 0.01, and uncertainty (±) consistently referred to 95% confidence or quantile intervals in the subsequent sections. To evaluate differences in production between tides, two-tailed *t* tests were employed. Pairwise comparisons of means were carried out using Duncan's multiple range test. In cases where significant differences were identified, the rank order was determined using Tukey's studentized range. Linear regressions were conducted using the 'lm' function.

Preprints (www.preprints.org) | NOT PEER-REVIEWED | Posted: 1 October 2023 doi:10.20944/preprints202310.0015.v1

3. Results

3.1. Environmental conditions

3.1.1. TE

We found that the predicted daily maximum tidal elevation (TE) based on the Hengsha tidal station matched the observed daily maximum TE in the creek fairly well (slope = 0.702, R^2 = 0.745) (Figure 2a). Additionally, it appeared that the estimation slightly overestimated TE, particularly during the winter months. It was not surprising that there was a linear relationship between the observed daily maximum TE and tidal duration (Figure 2b). Consequently, both the daily maximum TE and tidal duration can be used to measure the size and strength of tides. In practice, we used only the tide height simply because it could be more accurately measured using a scale.

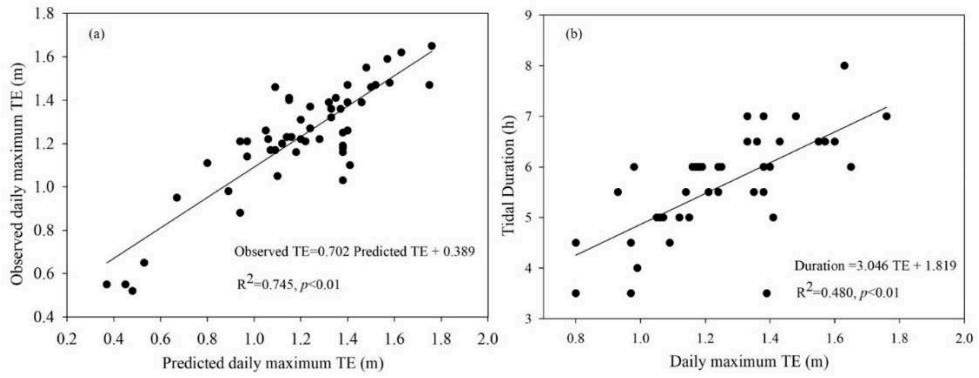

Figure 2. Linear relationships between observed daily maximum tidal elevation (TE) in the creek and the predicted daily maximum TE based on the Hengsha tidal station in 2010 (a), as well as between observed daily maximum TE and tidal duration (b).

3.1.2. Other factors

At both sites H and L, there was a weak correlation between evapotranspiration (ET) and the enhanced vegetation index (EVI) (ET=490.04EVI + 407.59, R^2=0.329) (Figure 3a). Furthermore, the R^2 value of 0.329 implied that there were likely other factors influencing ET beyond just EVI, such as tidal activities and land surface water content. The differences in GPP from eddy covariance towers (ΔGPP_{EC}) indicated the measured lateral response to TE, while the differences in MODIS-based gross primary production (GPP) (ΔGPP_{MODIS}) represented the predicted lateral response to TE. The strong correlation between ΔGPP_{EC} and ΔGPP_{MODIS} suggested that significant tidal influences at both sites might have occurred on lateral mass exchange (e.g., C flux) (Figure 3b).

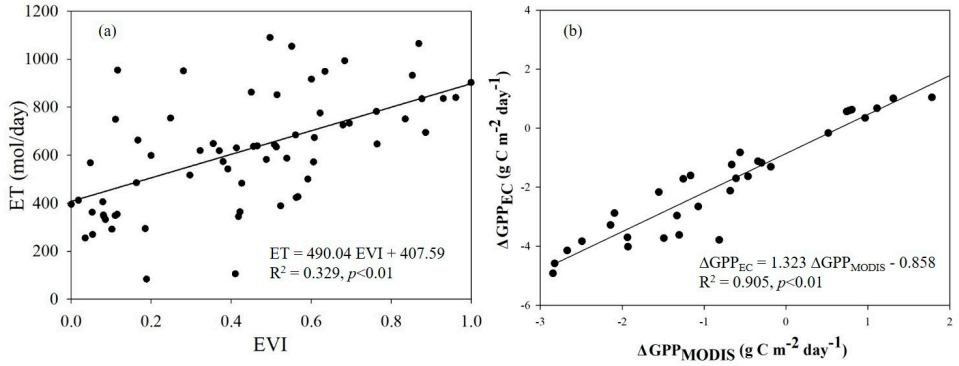

Figure 3. Simple linear relationships between evapotranspiration (ET) and the enhanced vegetation index (EVI) (a), and simple linear relationships between the differences in MODIS-based gross primary production (GPP) (ΔGPP_{MODIS}) and the differences in GPP from eddy covariance towers (ΔGPP_{EC}) at two sites (the high-elevation site: 31°31.000′N, 121°57.643′E, and the low-elevation site: 31°31.014′N, 121°58.300′E) for the 2010 growing season (b).

Preprints (www.preprints.org) | NOT PEER-REVIEWED | Posted: 1 October 2023 doi:10.20944/preprints202310.0015.v1

3.2. Lateral hydrological C/N fluxes

3.2.1. C flux

Overall, our one-year study revealed that the estimated mean annual DTC concentration was approximately 22.49 mg C L^{-1}, and it also showed a significant correlation in hydrological DTC between imports and exports (Figure 4a). In addition to the bidirectional lateral hydrological DTC flux resulting from tidal activities, C imported during flood tides that eventually found its way into the outputs also contributed to an increase in lateral hydrological C flux. Pairwise comparisons demonstrated that significantly more DTC was transported out than was brought in at the sampling locations and during the trips. As a result, this study confirmed that the saltmarsh under investigation primarily acted as a net exporter of DTC. Furthermore, except for a few instances of high concentration data during the growing seasons, we did not observe clear seasonality in ΔDTC during the experimental period. However, it is essential to note that we did not find a significant relationship between daily maximum relative tide elevations (RTE) and ΔDTC for the entire study period (Figure 4b).

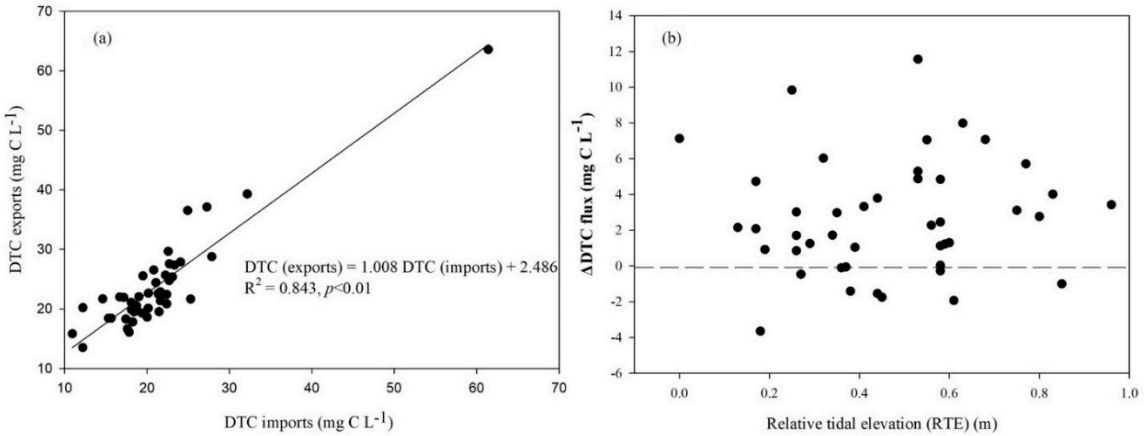

Figure 4. Linear relationship of dissolved total C (DTC) flows between imports and exports (a) and the daily net DTC fluxes under different relative tidal elevations (RTE) through the tidal creek in 2010 in the Dongtan wetlands, Shanghai, China (b). (ΔDTC = $DTC_{exports}$-DTC_{imprts}, where positive values indicate net fluxes out of the marsh and negative values indicate net fluxes into the marsh).

3.2.2. N flux

Net DTN fluxes (ΔDTN) per daily tidal cycle remained negative (i.e., a net flow into the marsh), differing in this respect from net DTC (ΔDTC) (Figure 5b). Furthermore, the ΔDTN fluxes during the daily tidal cycles ranged from –0.98 mg N L^{-1} to 0.27 mg N L^{-1}. In summary, our study has demonstrated that the estimated mean annual DTN concentration was ~ 1.26 mg N L^{-1}, and it has also shown that hydrological DTN fluxes between ebbing and flooding tidal waters exhibited a similar correlation to DTC (Figure 5a). Notably, this studied saltmarsh acted as a sink for DTN, implying a net DTN flow into the saltmarsh, rather than the accumulation of hydrological DTN in coastal wetlands. Furthermore, there was no significant difference in ΔDTN in the daily maximum relative tide elevation (RTE) sensitivity among the years (Figure 5b).

Preprints (www.preprints.org) | NOT PEER-REVIEWED | Posted: 1 October 2023 doi:10.20944/preprints202310.0015.v1

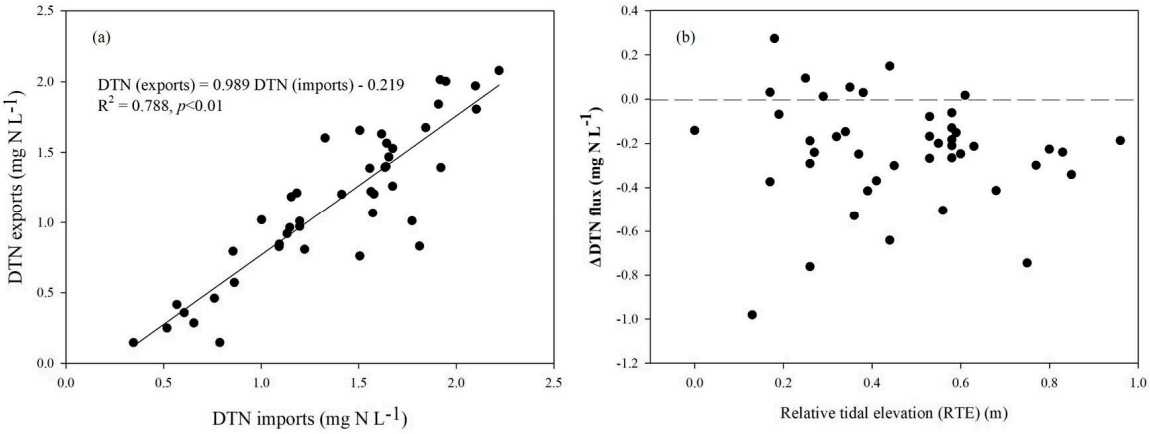

Figure 5. Linear relationship of dissolved total N (DTN) flows between imports and exports (a) and the daily net N fluxes under different relative tidal elevations (RTE) through the tidal creek in 2010 in the Dongtan wetlands, Shanghai, China (b). (ΔDTN = $DTN_{exports}$-DTN_{imprts}, where positive values indicate net fluxes out of the marsh and negative values indicate net fluxes into the marsh).

3.2.3. C/N ratio

Figure 6 shows that the total dissolved C/N ratio was also quite variable, ranging from a low value of 9.05 to a high value of 148.16. On average, the estimated hydrological C/N ratio in ebbs was approximately 30.19, with two exceptionally high peak ratios in March (i.e., 142.05 on DOY 62) and July (i.e., 148.16 on DOY 192). Notably, the C/N ratio in both floods and ebbs varied by month, but it was unaffected by sampling RTE (Figure 6b). However, on the other hand, there was a significant correlation in the total dissolved stoichiometry of the C/N ratio between imports and exports (Figure 6a).

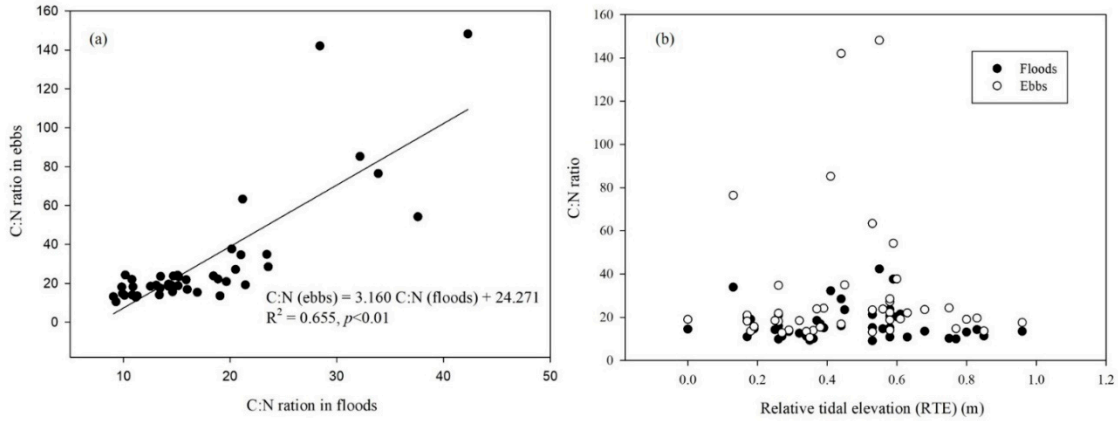

Figure 6. Linear relationship of hydrological C/N ratios between imports and exports (a) and their distributions under different relative tidal elevations (RTE) through the tidal creek in 2010 in the Dongtan wetlands, Shanghai, China (b).

4. Discussion

4.1. Uncertainties and challenges in cross-ecosystem flows

We emphasized the significance of lateral hydrological C/N fluxes in coastal marshes within the framework of the terrestrial-aquatic continuum, highlighting a thorough examination of the C/N ratio (Gülzow et al., 2018). Considering the technical challenges associated with obtaining direct measurements in wetlands characterized by a flow-through hydrologic regime, there is a need to develop and standardize indirect methods that integrate estimates of the diverse variables and processes associated with cross-ecosystem flows (Ganju et al., 2019). For instance, innovative

methods for estimating lateral C fluxes were devised to accommodate fluctuations in terrestrial GPP (Yang et al., 2023). These methods enabled us to predict the lateral C export of marshes when direct measurements were not feasible (Hawman et al., 2023). More importantly, ensuring accurate regional extrapolations from plot measurements to whole-marsh estimates relies on the precise estimation of terrestrial GPP and the assumption that plots are representative of the entire marsh (Liao et al., 2023). In contrast to previous studies conducted in nonwetland ecosystems, we reported in our earlier study a substantial underestimation of GPP when using the predicted GPP from the Light Use Efficiency (LUE) model (GPP_{MODIS}) in comparison to the GPP observed from eddy flux tower measurements (GPP_{EC}) (Yan et al., 2008). We attributed this underestimation to the influence of lateral C flux induced by tides, as well as CH_4 emissions (Gao et al., 2018). Our study also underscored the importance of exploring and evaluating cost-effective monitoring systems to address various sources of uncertainty in cross-ecosystem flows, including methodological design and analytical statistics (Gao et al., 2020). Therefore, we advocate for the prompt development of robust model frameworks when direct measurements are impractical. These frameworks are particularly essential for effectively estimating and mitigating uncertainties stemming from diverse sources (e.g., astronomical tides, water temperature and seasonal variations in sea level) (Alongi 2020).

The findings presented in this study highlight the difficulties involved in upscaling from field measurements to MODIS-based estimates. This challenge is likely to persist in future extrapolations based on tower-based measurements and MODIS time-series data (Tao et al., 2018). Consequently, there is a pressing need for methodological advancements to assess cross-ecosystem flows in scenarios where ecosystems exhibit less contrast (Alongi 2022). Fortunately, our initial efforts have shown a significant correlation between the predicted and observed environmental conditions, such as the daily maximum TE (Figure 2). Given that the relationship between lateral flux and TE can offer approximate estimates, it is pragmatic to acquire extensive time-series data on tidal hydrodynamics across various weather conditions (Yao et al., 2022). Subsequently, these data can be used for modeling and forecasting storm-driven lateral transport mechanisms. Consequently, primary tide-driven processes can be regarded as the primary mechanism for integrating tidal waves into the estuarine C budget of meta-ecosystems (Kim et al., 2020). However, another challenge in the meta-ecosystem framework lies in the infrequent consideration of storm conditions by researchers. This is primarily because it is challenging to obtain results under extreme weather conditions, such as during a severe storm when the highest transports almost always occur at the daily scale (Dhillon and Inamdar 2014). Storms, such as typhoons, were absent during the sampling period. Consequently, we were unable to capture the extent of lateral C flux generated during storm surges. Nevertheless, previous research has demonstrated the importance of comprehending and modeling the stability of hydrological C transport induced by storm tides in the context of lateral C flux (Call et al., 2019). In general, even though there are gaps in our knowledge and significant uncertainty in quantifying lateral mass export, we should also account for the role of estuarine animals in contributing to lateral ross-ecosystem flows, which are stored in the marsh and become part of the marsh C/N cycle. This contribution could enhance the availability of nutrients for incorporation into food chains/webs (Jinks et al., 2020).

4.2. Importance and implications of coupling C/N fluxes

This study emphasizes the lateral exchange of C and N across the terrestrial-aquatic continuum and underscores how their interconnected effects facilitate the connection of material flows, energy dynamics, and biological interactions within coastal ecosystems (Cheng et al., 2022). The reciprocal lateral C and N flows within ecosystems represent interconnected processes that mutually couple each other (Liu et al., 2020a). The spatial dynamics of C and N encompass the dynamic processes within ecosystems, linking various ecosystems and portraying the ecological processes and patterns of change influenced by ecosystem structure and function (Regier et al., 2021). This comprehension is vital for recognizing potential primary factors driving ecosystems. For example, it was discovered that over 50% of the annual net primary production (NPP) (approximately 506~1995 g C m^{-2}) in intertidal wetland ecosystems along the western coast of North America was transported to nearby

aquatic environments (Hyndes et al., 2014). The impact of dissolved organic matter on lateral fluxes in coastal wetlands indirectly alters community structure and composition, resulting in modifications to both ecosystem structure and function. This phenomenon has become a focal point in current research on lateral C flux (Akhand et al., 2021). For instance, an analysis of the global C outwelling from estuaries to the nearshore revealed a strong correlation with the productivity levels of adjacent fisheries (including invertebrates and fish) (Igulu et al., 2013). Additionally, lateral N flux encompasses the lateral movement and transformation of N elements within coastal ecosystems, involving nutrient exchange and transfer driven by tidal activities(Wang et al., 2023). For example, tidal hydrological processes create a conduit for aquatic organisms to access coastal wetlands for activities such as feeding, excretion, and reproduction, thereby facilitating nutrient transfer and material cycling (Marleau et al., 2020). Thus, by analyzing hydrological processes in coastal wetlands, such as TE, tidal flow velocity, and inundation duration, it is possible to assess how the spatial patterns of fish trophic elements (e.g., plankton, benthic organisms) directly or indirectly influence the structure of fish communities (Igulu et al., 2013).

Our findings also highlight the importance of incorporating ecological stoichiometric principles to better understand the intricate interrelationships between physical, chemical, and biological processes and how they respond to land-to-ocean aquatic continuum fluxes (Regnier et al., 2022). Coastal wetlands exhibit intricate patterns of C/N ratios in their exchange of materials with neighboring water bodies (Lamb et al., 2006). Notably, an increasing body of evidence emphasizes the critical importance of investigating changes in stoichiometric ratios, particularly the C/N ratio within ecosystems (Sardans et al., 2012). Furthermore, it has been indicated that both C outwelling and N exchanges occur concurrently, implying a bidirectional nutritional process (Lu et al., 2023a). To study the coupling models of the C/N ratio, it is necessary to first examine the influence of lateral C flux on C and N cycles at the ecosystem scale and the impact of lateral N fluxes on these cycles (Wang et al., 2023). Due to the similarity in the C/N ratio between marine and terrestrial ecosystems, for example, increasing the size of the nearshore C pool also increases the size of the nearshore N pool (Gülzow et al., 2018). On the other hand, it was found that lateral N input from the nearshore significantly increased the NPP of coastal salt marshes and increased C and N storage in saltmarsh vegetation (Li et al., 2022). These research findings indicate that increasing lateral C flux significantly promotes C and N retention within ecosystems, and increasing lateral N input also promotes the growth of saltmarsh vegetation and the accumulation of C and N in vegetation and litter (Leroux et al., 2017). Thus, investigating the reciprocal lateral C and N flows at terrestrial-aquatic interfaces is essential for understanding their influence on C and N cycling (Xu et al., 2013). These reciprocal interactions are crucial in maintaining and regulating energy balance and material cycling in coastal and estuarine ecosystems. Both modeling assessments and field investigations have yielded evidence supporting the need to explore the driving mechanisms behind spatial variations in C and nutrient transport within the context of human activities and climate change (Regnier et al., 2013). Therefore, conducting concurrent investigations into coupling C/N fluxes can offer a more holistic grasp of the interconnected material flow dynamics within coastal wetlands (Gao et al., 2014). Additionally, it is important to integrate the ecological stoichiometry laws governing coupled C and N cycles and their systemic driving forces (Shousha et al., 2021).

4.3. Extension and limitation of rooting meta-ecosystems

This study emphasizes the impact of spatial flows on meta-ecosystems and provides a straightforward way to predict these effects using a connectivity measure (Newton et al., 2020). Our findings have revealed that when considering reciprocal hydrological lateral C and N flows, single ecosystems can function as both sources and sinks within the meta-ecosystem framework (Figure 7) (Gravel et al., 2010). In the meta-ecosystem framework, the transfer and modification of resource flows driven by tidal movements, along with dispersal-based connections between these ecosystems, result in even larger-scale exchanges between ecosystems (Justić et al., 2022). Furthermore, these dynamics can have feedback effects on dispersal-based meta-ecosystems and resource-flow-based meta-ecosystems and underscore the significance of balancing the C/N budget within coastal

Preprints (www.preprints.org) | NOT PEER-REVIEWED | Posted: 1 October 2023 doi:10.20944/preprints202310.0015.v1

wetlands in the context of the terrestrial–aquatic continuum (Limberger et al., 2017). For example, the nutrient-explicit model was introduced and applied to explore the importance of nutrient cycling and diffusion in shaping the dynamics of meta-ecosystems (Marleau et al., 2015). Their subsequent model development offered a clear framework for comprehending the dynamic relationships between biotic and abiotic factors across various spatial and temporal scales within coastal wetlands (Angus 2018). Furthermore, the development of the meta-ecosystem framework enables a more accurate quantification of spatial flows associated with biological movements (such as dispersion, life cycles, and migration), feedback mechanisms, and resource dynamics (Gounand et al., 2018). Advancements in tracking aquatic animal migrations, monitoring technologies for terrestrial-to-aquatic environmental transitions, and the establishment of observation facilities for horizontal C exchange in coastal wetlands have addressed significant gaps in our understanding of the spatial scales relevant to migration types and the material fluxes associated with these movements (Soininen et al., 2015). In addition, coastal wetland C and N cycling may vary among years; therefore, multiyear data are needed to assess the extent to which these hydrological fluxes and their lateral budgets contribute to the differences between terrestrial-aquatic meta-ecosystems over the long term (Bittar et al., 2016).

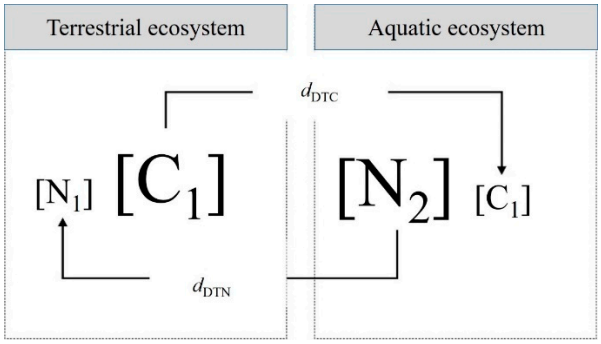

Figure 7. Schematic illustrating the dynamics of lateral hydrological C/N flows in a source-sink meta-ecosystem at a terrestrial–aquatic interface. N represents the equilibrium DTN amount, and C represents the equilibrium DTC amount. Character size corresponds to concentration.

To answer ecosystem-level questions in spatial ecology, the meta-ecosystem perspective provides a powerful theoretical framework to understand the mechanism of the recipient intertidal environment (Zhu et al., 2022). However, it should be noted that it encompasses only various spatial flows of hydrological C/N flows between systems in this study. As a natural extension of the concepts of meta-populations and meta-communities, the concept of a meta-ecosystem focuses on spatial processes at the entire ecosystem level (Loreau et al., 2003). It encompasses not only the dispersal of organisms but also the constraints and feedback mechanisms imposed by abiotic factors, such as particulate flows and detritus flows. Exploring the source/sink attributes and process mechanisms through landscape connectivity spatial models and cross-ecosystem processes can help us understand the coupled mechanisms between physical processes, chemical processes, and biological processes (Gravel et al., 2010). For example, the spatial utilization patterns of habitats by species during various migration activities, such as spawning, juvenile rearing, overwintering, and migration, can be driven by organism flows (Tamario et al., 2019). The dynamics of coastal ecosystems are influenced not only by diffusion from source/sink attributes but also by the reproductive capacity and community structure of aquatic organisms responsible for spatial nutrient and energy flows in adjacent ecosystems (Angeler et al., 2023). For example, the hydrodynamics of changes in the spatial patterns of fish trophic elements can serve as an ecosystem driver, linking functional connectivity spatial models and ecological processes (Wootton et al., 2023). Likewise, plant-derived detritus subject to frequent inundation and influenced by plant-mediated convective flow might undergo a transition into microbial food webs along a potential continuum, driven by interactions with rich organic matter and concentrated nutrients (Duarte et al., 2014). Furthermore, novel approaches that integrate the capabilities of isotope data for documenting and tracking temporal trophic cascades in the estimation of cross-ecosystem flows could also be improved by

considering the influence of spatial flows (Ray et al., 2018). The presence or absence of spatial flows in coastal wetlands may lead to divergent impacts on the provision of ecosystem services and the preservation of suitable levels of connectivity and functionality in the landscape (Hillman et al., 2018). Thus, enhancing our capacity to predict alterations in interconnected ecosystems across temporal and spatial scales that encompass shifts in hydrological regimes is an evident priority for future research (Zhang et al., 2023). In a natural setting, we can investigate whether the transition between different nutrient flows occurs within the framework of a novel integrated spatial ecosystem ecology approach (Jacquet et al., 2022).

5. Conclusions

Field observations and model estimates of lateral hydrological C and N fluxes have traditionally been studied separately. When considering cross-system flows on broad spatial scales, we argue that both remote sensing-based GPP and EC tower-based GPP should be more extensively considered as potential predictors of lateral hydrological nutrient budgets. The predicted daily maximum TE closely matched the observed values in the creek. The strong correlation between ΔGPP_{EC} and ΔGPP_{MODIS} suggests substantial tidal influences at both sites affecting lateral mass exchange. Our study indicates that the saltmarsh studied acts as a net exporter of DTC while serving as a net sink for DTN. We observed a significant correlation in the total dissolved stoichiometry of the C/N ratio between imports and exports. Our findings also stress the value of integrating ecological stoichiometric principles to gain a deeper understanding of the complex relationships between physical, chemical, and biological processes and their responses to land-to-ocean aquatic continuum fluxes. Moreover, when considering reciprocal hydrological lateral C and N flows, single ecosystems can function both as sources and sinks within rooting the meta-ecosystem framework.

Author Contributions: Conceptualization, Y.G. and B.Z.; methodology, Y.G. and B.Z.; software, W.W.; validation, Y.G.; formal analysis, C.S.; investigation, Y.G., Z.G. and G.Y.; resources, F.Z. and T.Z.; data curation, Y.G.; writing—original draft preparation, Y.G.; writing—review and editing, Y.G., M.M. and L.W.; visualization, W.W.; supervision, B.Z., N.S. and P.Z.; project administration, F.Z.; funding acquisition, B.Z. and P.Z. All authors have read and agreed to the version of the manuscript.

Funding: This work received support from the Foundation of Key Laboratory of Yangtze River Water Environment, Ministry of Education (Tongji University), China (No. YRWEF202105), the Natural Science Foundation of China (Grant No. 32271658), the Central Public-Interest Scientific Institution Basal Research Fund, CAFS (Grant NO. 2020TD13), and the Natural Science Fund of Shanghai (Grant NO. 19ZR1470300).

Data Availability Statement: The data presented in this study are available on request from the corresponding author.

Acknowledgments: We are grateful to our student assistants for their help during fieldwork. The first author expresses gratitude to the China Scholarship Council (CSC) for providing a scholarship at Macquarie University. This paper is a contribution of the 'meta-communities' working group at the US-China Carbon Consortium (USCCC).

Conflicts of Interest: The authors declare no conflict of interest.

References

Akhand, A., Watanabe, K., Chanda, A., Tokoro, T., Chakraborty, K., Moki, H., Tanaya, T., Ghosh, J., Kuwae, T., 2021. Lateral carbon fluxes and CO_2 evasion from a subtropical mangrove-seagrass-coral continuum. Sci Total Environ. **752**, 142190.

Alongi, D. M., 2020. Carbon balance in salt marsh and mangrove ecosystems: A global synthesis. Journal of Marine Science and Engineering. **8**, 767.

Alongi, D. M., 2022. Lateral export and sources of subsurface dissolved carbon and alkalinity in mangroves: Revising the blue carbon budget. Journal of Marine Science and Engineering. **10**, 1916.

Angeler, D. G., Heino, J., Rubio-Ríos, J., Casas, J. J., 2023. Connecting distinct realms along multiple dimensions: A meta-ecosystem resilience perspective. Sci Total Environ. **889**, 164169.

Angus, S., 2018. Beyond the meta-ecosystem? The need for a multi-faceted approach to climate change planning on coastal wetlands: An example from South Uist, Scotland. Ocean & Coastal Management. **165**, 334-345.

Bittar, T. B., Berger, S. A., Birsa, L. M., Walters, T. L., Thompson, M. E., Spencer, R. G. M., Mann, E. L., Stubbins, A., Frischer, M. E., Brandes, J. A., 2016. Seasonal dynamics of dissolved, particulate and microbial components of a tidal saltmarsh-dominated estuary under contrasting levels of freshwater discharge. Estuarine, Coastal and Shelf Science. **182**, 72-85.

Call, M., Sanders, C. J., Macklin, P. A., Santos, I. R., Maher, D. T., 2019. Carbon outwelling and emissions from two contrasting mangrove creeks during the monsoon storm season in Palau, Micronesia. Estuar Coast Shelf S. **218**, 340-348.

Casas-Ruiz, J. P., Bodmer, P., Bona, K. A., Butman, D., Couturier, M., Emilson, E. J. S., Finlay, K., Genet, H., Hayes, D., Karlsson, J., Paré, D., Peng, C., Striegl, R., Webb, J., Wei, X., Ziegler, S. E., del Giorgio, P. A., 2023. Integrating terrestrial and aquatic ecosystems to constrain estimates of land-atmosphere carbon exchange. Nature Communications. **14**, 1571.

Cheng, D., Minquan, F., Yibo, W., Xiaoge, D., 2022. Spatial variation of the C: N ratio and its relationship with the carbon cycle in the middle reaches of the Yellow River during summer. Chemistry and Ecology. **38**, 841-856.

Clark, J. B., Long, W., Hood, R. R., 2020. A comprehensive estuarine dissolved organic carbon budget using an enhanced biogeochemical model. Journal of Geophysical Research: Biogeosciences. **125**, e2019JG005442.

Covino, T., 2017. Hydrologic connectivity as a framework for understanding biogeochemical flux through watersheds and along fluvial networks. Geomorphology. **277**, 133-144.

Das, A., Justic, D., Swenson, E., Turner, R. E., Inoue, M., Park, D., 2011. Coastal land loss and hypoxia: the 'outwelling' hypothesis revisited. Environ Res Lett. **6**.

Dhillon, G. S., Inamdar, S., 2014. Storm event patterns of particulate organic carbon (POC) for large storms and differences with dissolved organic carbon (DOC). Biogeochemistry. **118**, 61-81.

Duarte, B., Valentim, J. M., Dias, J. M., Silva, H., Marques, J. C., Caçador, I., 2014. Modelling sea level rise (SLR) impacts on salt marsh detrital outwelling C and N exports from an estuarine coastal lagoon to the ocean (Ria de Aveiro, Portugal). Ecol Model. **289**, 36-44.

Ganju, N. K., Defne, Z., Elsey-Quirk, T., Moriarty, J. M., 2019. Role of tidal wetland stability in lateral fluxes of particulate organic matter and carbon. Journal of Geophysical Research: Biogeosciences. **124**, 1265-1277.

Gao, Y., Chen, J., Saintilan, N., Zhao, B., Ouyang, Z., Zhang, T., Guo, H., Hao, Y., Zhao, F., Liu, J., Wang, S., Zhuang, P., 2023. Integrating monthly spring tidal waves into estuarine carbon budget of meta-ecosystems. Sci Total Environ. **905**, 167026.

Gao, Y., Chen, J., Zhang, T., Zhao, B., McNulty, S., Guo, H., Zhao, F., Zhuang, P., 2021. Lateral detrital C transfer across a *Spartina alterniflora* invaded estuarine wetland. Ecological Processes. **10**, 70.

Gao, Y., Ouyang, Z. T., Shao, C. L., Chu, H. S., Su, Y. J., Guo, H. Q., Chen, J. Q., Zhao, B., 2018. Field observation of lateral detritus carbon flux in a coastal wetland. Wetlands. **38**, 613-625.

Gao, Y., Peng, R.-H., Ouyang, Z.-T., Shao, C.-L., Chen, J.-Q., Zhang, T.-T., Guo, H.-Q., Tang, J.-W., Zhao, F., Zhuang, P., Zhao, B., 2020. Enhanced lateral exchange of carbon and nitrogen in a coastal wetland with invasive *Spartina alterniflora*. Journal of Geophysical Research: Biogeosciences. **125**, e2019JG005459.

Gao, Y., Zhu, B., Yu, G., Chen, W., He, N., Wang, T., Miao, C., 2014. Coupled effects of biogeochemical and hydrological processes on C, N, and P export during extreme rainfall events in a purple soil watershed in southwestern China. J Hydrol. **511**, 692-702.

Gounand, I., Harvey, E., Little, C. J., Altermatt, F., 2018. Meta-ecosystems 2.0: Rooting the theory into the field. Trends Ecol Evol. **33**, 36-46.

Gravel, D., Guichard, F., Loreau, M., Mouquet, N., 2010. Source and sink dynamics in meta-ecosystems. Ecology. **91**, 2172-2184.

Gülzow, N., Wahlen, Y., Hillebrand, H., 2018. Metaecosystem dynamics of marine phytoplankton alters resource use efficiency along stoichiometric gradients. The American Naturalist. **193**, 35-50.

Guo, H. Q., Noormets, A., Zhao, B., Chen, J. Q., Sun, G., Gu, Y. J., Li, B., Chen, J. K., 2009. Tidal effects on net ecosystem exchange of carbon in an estuarine wetland. Agr Forest Meteorol. **149**, 1820-1828.

Harvey, E., Marleau, J. N., Gounand, I., Leroux, S. J., Firkowski, C. R., Altermatt, F., Guillaume Blanchet, F., Cazelles, K., Chu, C., D'Aloia, C. C., Donelle, L., Gravel, D., Guichard, F., McCann, K., Ruppert, J. L. W., Ward, C., Fortin, M.-J., 2023. A general meta-ecosystem model to predict ecosystem functions at landscape extents. Ecography. e06790.

Hawman, P. A., Mishra, D. R., O'Connell, J. L., 2023. Dynamic emergent leaf area in tidal wetlands: Implications for satellite-derived regional and global blue carbon estimates. Remote Sensing of Environment. **290**, 113553.

Hillman, J. R., Lundquist, C. J., Thrush, S. F., 2018. The challenges associated with connectivity in ecosystem processes. Front Mar Sci. **5**, 364.

Huang, Y., Chen, Z., Tian, B., Zhou, C., Wang, J., Ge, Z., Tang, J., 2020. Tidal effects on ecosystem CO_2 exchange in a Phragmites salt marsh of an intertidal shoal. Agr Forest Meteorol. **292-293**, 108108.

Hyndes, G. A., Nagelkerken, I., McLeod, R. J., Connolly, R. M., Lavery, P. S., Vanderklift, M. A., 2014. Mechanisms and ecological role of carbon transfer within coastal seascapes. Biological Reviews. **89**, 232-254.

Igulu, M. M., Nagelkerken, I., van der Velde, G., Mgaya, Y. D., 2013. Mangrove fish production is largely fuelled by external food sources: A stable isotope analysis of fishes at the individual, species, and community levels from across the globe. Ecosystems. **16**, 1336-1352.

Jacquet, C., Carraro, L., Altermatt, F., 2022. Meta-ecosystem dynamics drive the spatial distribution of functional groups in river networks. Oikos. **2022**, e09372.

Jeong, Y.-J., Park, H.-J., Baek, N., Seo, B.-S., Lee, K.-S., Kwak, J.-H., Choi, S.-K., Lee, S.-M., Yoon, K.-S., Lim, S.-S., Choi, W.-J., 2023. Assessment of sources variability of riverine particulate organic matter with land use and rainfall changes using a three-indicator ($\delta^{13}C$, $\delta^{15}N$, and C/N) Bayesian mixing model. Environmental Research. **216**, 114653.

Jinks, K. I., Rasheed, M. A., Brown, C. J., Olds, A. D., Schlacher, T. A., Sheaves, M., York, P. H., Connolly, R. M., 2020. Saltmarsh grass supports fishery food webs in subtropical Australian estuaries. Estuarine, Coastal and Shelf Science. **238**, 106719.

Justić, D., Kourafalou, V., Mariotti, G., He, S., Weisberg, R., Androulidakis, Y., Barker, C., Bracco, A., Dzwonkowski, B., Hu, C., Huang, H., Jacobs, G., Le Hénaff, M., Liu, Y., Morey, S., Nittrouer, J., Overton, E., Paris, C. B., Roberts, B. J., Rose, K., Valle-Levinson, A., Wiggert, J., 2022. Transport processes in the Gulf of Mexico along the river-estuary-shelf-ocean continuum: A review of research from the Gulf of Mexico research initiative. Estuar Coast. **45**, 621-657.

Kim, J., Blair, N. E., Ward, A. S., Goff, K., 2020. Storm-induced dynamics of particulate organic carbon in clear creek, iowa: An intensively managed landscape critical zone observatory story. Frontiers in Water. **2**, 578261.

Lamb, A. L., Wilson, G. P., Leng, M. J., 2006. A review of coastal palaeoclimate and relative sea-level reconstructions using $\delta^{13}C$ and C/N ratios in organic material. Earth-Science Reviews. **75**, 29-57.

Leroux, S. J., Wal, E. V., Wiersma, Y. F., Charron, L., Ebel, J. D., Ellis, N. M., Hart, C., Kissler, E., Saunders, P. W., Moudrá, L., Tanner, A. L., Yalcin, S., 2017. Stoichiometric distribution models: ecological stoichiometry at the landscape extent. Ecology Letters. **20**, 1495-1506.

Li, H., Dai, S. Q., Ouyang, Z. T., Xie, X., Guo, H. Q., Gu, C. H., Xiao, X. M., Ge, Z. M., Peng, C. H., Zhao, B., 2018. Multi-scale temporal variation of methane flux and its controls in a subtropical tidal salt marsh in eastern China. Biogeochemistry. **137**, 163-179.

Li, S., Luo, J., Xu, Y. J., Zhang, L., Ye, C., 2022. Hydrological seasonality and nutrient stoichiometry control dissolved organic matter characterization in a headwater stream. Sci Total Environ. **807**, 150843.

Liao, Z., Zhou, B., Zhu, J., Jia, H., Fei, X., 2023. A critical review of methods, principles and progress for estimating the gross primary productivity of terrestrial ecosystems. Front Env Sci-Switz. **11**, 1093095.

Limberger, R., Birtel, J., Farias, D. d. S., Matthews, B., 2017. Ecosystem flux and biotic modification as drivers of metaecosystem dynamics. Ecology. **98**, 1082-1092.

Lin, J., Hu, A., Wang, F., Hong, Y., Krom, M. D., Chen, N., 2023. Impacts of a subtropical storm on nitrogen functional microbes and associated cycling processes in a river-estuary continuum. Sci Total Environ. **861**, 160698.

Liu, Q., Liang, Y., Cai, W.-J., Wang, K., Wang, J., Yin, K., 2020a. Changing riverine organic C:N ratios along the Pearl River: Implications for estuarine and coastal carbon cycles. Sci Total Environ. **709**, 136052.

Liu, Y.-F., Ma, J., Wang, X.-X., Zhong, Q.-Y., Zong, J.-M., Wu, W.-B., Wang, Q., Zhao, B., 2020b. Joint effect of *Spartina alterniflora* invasion and reclamation on the spatial and temporal dynamics of tidal flats in Yangtze River estuary. Remote Sensing. **12**, 1725.

Loreau, M., Mouquet, N., Holt, R. D., 2003. Meta-ecosystems: A theoretical framework for a spatial ecosystem ecology. Ecology Letters. **6**, 673-679.

Lu, X., Wang, C., Lao, Q., Jin, G., Chen, F., Zhou, X., Chen, C., 2023a. Interactions between particulate organic matter and dissolved organic matter in a weak dynamic bay revealed by stable isotopes and optical properties. Front Mar Sci. **10**, 1144818.

Lu, Z., Wang, F., Xiao, K., Wang, Y., Yu, Q., Cheng, P., Chen, N., 2023b. Carbon dynamics and greenhouse gas outgassing in an estuarine mangrove wetland with high input of riverine nitrogen. Biogeochemistry. **162**, 221-235.

Lu, Z., Xiao, K., Wang, F., Wang, Y., Yu, Q., Chen, N., 2023c. Salt marsh invasion reduces recalcitrant organic carbon pool while increases lateral export of dissolved inorganic carbon in a subtropical mangrove wetland. Geoderma. **437**, 116573.

Makings, U., Santos, I. R., Maher, D. T., Golsby-Smith, L., Eyre, B. D., 2014. Importance of budgets for estimating the input of groundwater-derived nutrients to an eutrophic tidal river and estuary. Estuar Coast Shelf S. **143**, 65-76.

Marleau, J. N., Guichard, F., Loreau, M., 2015. Emergence of nutrient co-limitation through movement in stoichiometric meta-ecosystems. Ecology Letters. **18**, 1163-1173.

Marleau, J. N., Peller, T., Guichard, F., Gonzalez, A., 2020. Converting ecological currencies: Energy, material, and information flows. Trends Ecol Evol. **35**, 1068-1077.

McGroddy, M. E., Baisden, W. T., Hedin, L. O., 2008. Stoichiometry of hydrological C, N, and P losses across climate and geology: An environmental matrix approach across New Zealand primary forests. Global Biogeochem Cy. **22**, GB1026.

Moffat, A. M., Papale, D., Reichstein, M., Hollinger, D. Y., Richardson, A. D., Barr, A. G., Beckstein, C., Braswell, B. H., Churkina, G., Desai, A. R., Falge, E., Gove, J. H., Heimann, M., Hui, D., Jarvis, A. J., Kattge, J., Noormets, A., Stauch, V. J., 2007. Comprehensive comparison of gap-filling techniques for eddy covariance net carbon fluxes. Agr Forest Meteorol. **147**, 209-232.

Newton, A., Icely, J., Cristina, S., Perillo, G. M. E., Turner, R. E., Ashan, D., Cragg, S., Luo, Y., Tu, C., Li, Y., Zhang, H., Ramesh, R., Forbes, D. L., Solidoro, C., Béjaoui, B., Gao, S., Pastres, R., Kelsey, H., Taillie, D., Nhan, N., Brito, A. C., de Lima, R., Kuenzer, C., 2020. Anthropogenic, direct pressures on coastal wetlands. Frontiers in Ecology and Evolution. **8**, 144.

Ouyang, Z.-T., Gao, Y., Xie, X., Guo, H.-Q., Zhang, T.-T., Zhao, B., 2013. Spectral discrimination of the invasive plant *Spartina alterniflora* at multiple phenological stages in a saltmarsh wetland. PLOS ONE. **8**, e67315.

Ray, R., Michaud, E., Aller, R. C., Vantrepotte, V., Gleixner, G., Walcker, R., Devesa, J., Le Goff, M., Morvan, S., Thouzeau, G., 2018. The sources and distribution of carbon (DOC, POC, DIC) in a mangrove dominated estuary (French Guiana, South America). Biogeochemistry. **138**, 297-321.

Regier, P., Ward, N. D., Indivero, J., Moore, C. W., Norwood, M., Myers-Pigg, A., 2021. Biogeochemical control points of connectivity between a tidal creek and its floodplain. Limnol Oceanogr Lett. **6**, 134-142.

Regnier, P., Friedlingstein, P., Ciais, P., Mackenzie, F. T., Gruber, N., Janssens, I. A., Laruelle, G. G., Lauerwald, R., Luyssaert, S., Andersson, A. J., Arndt, S., Arnosti, C., Borges, A. V., Dale, A. W., Gallego-Sala, A., Goddéris, Y., Goossens, N., Hartmann, J., Heinze, C., Ilyina, T., Joos, F., LaRowe, D. E., Leifeld, J., Meysman, F. J. R., Munhoven, G., Raymond, P. A., Spahni, R., Suntharalingam, P., Thullner, M., 2013. Anthropogenic perturbation of the carbon fluxes from land to ocean. Nature Geoscience. **6**, 597-607.

Regnier, P., Resplandy, L., Najjar, R. G., Ciais, P., 2022. The land-to-ocean loops of the global carbon cycle. Nature. **603**, 401-410.

Sandoval-Gil, J. M., Avila-Lopez, M. D., Camacho-Ibar, V. F., Hernandez-Ayon, J., Zertuche-Gonzalez, J. A., Cabello-Pasini, A., 2019. Regulation of Nitrate Uptake by the Seagrass Zostera marina During Upwelling. Estuar Coast. **42**, 731-742.

Sardans, J., Rivas-Ubach, A., Peñuelas, J., 2012. The C:N:P stoichiometry of organisms and ecosystems in a changing world: A review and perspectives. Perspectives in Plant Ecology, Evolution and Systematics. **14**, 33-47.

Shousha, S., Maranger, R., Lapierre, J.-F., 2021. Different forms of carbon, nitrogen, and phosphorus influence ecosystem stoichiometry in a north temperate river across seasons and land uses. Limnol Oceanogr. **66**, 4285-4298.

Soininen, J., Bartels, P., Heino, J., Luoto, M., Hillebrand, H., 2015. Toward more integrated ecosystem research in aquatic and terrestrial environments. Bioscience. **65**, 174-182.

Taillardat, P., Ziegler, A. D., Friess, D. A., Widory, D., David, F., Ohte, N., Nakamura, T., Evaristo, J., Nguyen, T. N., Vinh, T. V., Marchand, C., 2019. Assessing nutrient dynamics in mangrove porewater and adjacent tidal creek using nitrate dual-stable isotopes: A new approach to challenge the outwelling hypothesis? Mar Chem. **214**, 103662.

Tamario, C., Sunde, J., Petersson, E., Tibblin, P., Forsman, A., 2019. Ecological and evolutionary consequences of environmental change and management actions for migrating fish. Frontiers in Ecology and Evolution. **7**, 271.

Tao, J., Mishra, D. R., Cotten, D. L., O'Connell, J., Leclerc, M., Nahrawi, H. B., Zhang, G., Pahari, R., 2018. A comparison between the MODIS product (MOD17A2) and a tide-robust empirical GPP model evaluated in a Georgia wetland. Remote Sensing. **10**, 1831.

Wang, Y., Lin, J., Wang, F., Tian, Q., Zheng, Y., Chen, N., 2023. Hydrological connectivity affects nitrogen migration and retention in the land–river continuum. Journal of Environmental Management. **326**, 116816.

Wootton, K. L., Curtsdotter, A., Bommarco, R., Roslin, T., Jonsson, T., 2023. Food webs coupled in space: Consumer foraging movement affects both stocks and fluxes. Ecology. **104**, e4101.

Wu, M., Muhammad, S., Chen, F., Niu, Z., Wang, C., 2015. Combining remote sensing and eddy covariance data to monitor the gross primary production of an estuarine wetland ecosystem in East China. Environmental Science: Processes & Impacts. **17**, 753-762.

Wu, W., Yang, Z., Chen, C., Tian, B., 2022. Tracking the environmental impacts of ecological engineering on coastal wetlands with numerical modeling and remote sensing. Journal of Environmental Management. **302**, 113957.

Xu, H., Chen, Z., Finlayson, B., Webber, M., Wu, X., Li, M., Chen, J., Wei, T., Barnett, J., Wang, M., 2013. Assessing dissolved inorganic nitrogen flux in the Yangtze River, China: Sources and scenarios. Global and Planetary Change. **106**, 84-89.

Yan, Y.-E., Guo, H.-Q., Gao, Y., Zhao, B., Chen, J.-Q., Li, B., Chen, J.-K., 2010. Variations of net ecosystem CO_2 exchange in a tidal inundated wetland: Coupling MODIS and tower-based fluxes. Journal of Geophysical Research: Atmospheres. **115**, D15102.

Yan, Y., Zhao, B., Chen, J., Guo, H., Gu, Y., Wu, Q., Li, B. O., 2008. Closing the carbon budget of estuarine wetlands with tower-based measurements and MODIS time series. Global Change Biology. **14**, 1690-1702.

Yang, Z., Huang, Y., Duan, Z., Tang, J., 2023. Capturing the spatiotemporal variations in the gross primary productivity in coastal wetlands by integrating eddy covariance, Landsat, and MODIS satellite data: A case study in the Yangtze Estuary, China. Ecological Indicators. **149**, 110154.

Yao, H. M., Montagna, P. A., Wetz, M. S., Staryk, C. J., Hu, X. P., 2022. Subtropical estuarine carbon budget under various hydrologic extremes and implications on the lateral carbon exchange from tidal wetlands. Water Res. **217**, 118436.

Zhang, H., Mächler, E., Morsdorf, F., Niklaus, P. A., Schaepman, M. E., Altermatt, F., 2023. A spatial fingerprint of land-water linkage of biodiversity uncovered by remote sensing and environmental DNA. Sci Total Environ. **867**, 161365.

Zhao, B., Guo, H., Yan, Y., Wang, Q., Li, B., 2008. A simple waterline approach for tidelands using multi-temporal satellite images: A case study in the Yangtze Delta. Estuar Coast Shelf S. **77**, 134-142.

Zhao, B., Yan, Y., Guo, H., He, M., Gu, Y., Li, B., 2009. Monitoring rapid vegetation succession in estuarine wetland using time series MODIS-based indicators: An application in the Yangtze River Delta area. Ecological Indicators. **9**, 346-356.

Zhu, P., Chen, X., Zhang, Y., Zhang, Q., Wu, X., Zhao, H., Qi, L., Shao, X., Li, L., 2022. Porewater-derived blue carbon outwelling and greenhouse gas emissions in a subtropical multi-species saltmarsh. Front Mar Sci. **9**, 884951.